ARTICLE

OBC
www.rsc.org/obc

Synthesis of (6*R*)- and (6*S*)-5,10-dideazatetrahydrofolate oligo-γ-glutamates: Kinetics of multiple glutamate ligations catalyzed by folylpoly-γ-glutamate synthetase†

John W. Tomsho,[a] John J. McGuire[b] and James K. Coward*[a]

[a] *Departments of Medicinal Chemistry and Chemistry, University of Michigan, 3813 Chemistry, 930 N. University, Ann Arbor, MI, 48109-1055, USA. E-mail: jkcoward@umich.edu; Fax: 734-647-4865*

[b] *Grace Cancer Drug Center, Roswell Park Cancer Institute, Buffalo, NY, 14263*

Received (Pittsburgh, PA, USA) 26th April 2005, Accepted 20th July 2005
First published as an Advance Article on the web 15th August 2005

Folylpoly-γ-glutamate synthetase (FPGS, EC 6.3.2.17) catalyzes the ATP-dependent ligation of glutamic acid to reduced folates including (6*S*)-5,6,7,8-tetrahydrofolate (H_4PteGlu), as well as to anticancer drugs such as 5,10-dideaza-5,6,7,8-tetrahydrofolate ((6*R*)-$DDAH_4PteGlu_1$, (6*R*)-DDATHF, Lometrexol™). Synthesis of unlabeled mono- and polyglutamates, $DDAH_4PteGlu_n$ (6*R*, $n = 1$–6; 6*S*, $n = 1$–2), as well as (6*R*)-$DDAH_4Pte[^{14}C]Glu_1$, was effected from (6*R*)- or (6*S*)-5,10-dideazatetrahydropteroyl azide and glutamic acid, H-Glu-γ-Glu_n-γ-Glu-OH ($n =$ 0–4), or [^{14}C]glutamic acid, respectively. These compounds were evaluated as FPGS substrates to determine steady-state kinetic constants. Michaelis–Menten kinetics were observed for (6*R*)-$DDAH_4PteGlu_1$, the isomer corresponding to H_4PteGlu, whereas marked substrate inhibition was observed for (6*S*)-$DDAH_4PteGlu_n$ ($n = 1$–2) and (6*R*)-$DDAH_4PteGlu_n$ ($n = 2$–5), but not (6*R*)-$DDAH_4PteGlu_6$. Multiple ligation of glutamate renders a quantitative analysis of these data difficult. However, approximate values of $K_M = 0.65$–1.6 μM and $K_I =$ 144–417 μM for $DDAH_4PteGlu_n$ were obtained using a simple kinetic model.

Introduction

Folylpoly-γ-glutamate synthetase (FPGS, EC 6.3.2.17) is the enzyme responsible for the intracellular poly-γ-glutamylation of natural folates as well as many antifolates (Scheme 1). This poly-γ-glutamylation leads to increased intracellular retention and (often) affinity for the target enzymes.[1–3] The antifolate (6*R*)-5,10-dideaza-5,6,7,8-tetrahydrofolate ((6*R*)-$DDAH_4PteGlu_1$, (6*R*)-DDATHF, LY264618, Lometrexol™) has been evaluated in clinical trials as a treatment for breast and non-small cell lung cancers as well as melanoma, sarcoma, and others.[4–7] $DDAH_4PteGlu_1$ is an inhibitor of *de novo* purine biosynthesis that specifically inhibits the reaction catalyzed by glycinamide ribonucleotide formyltransferase (GARFT, EC 2.1.2.1).[8] The (6*R*)- and (6*S*)-diastereomers of $DDAH_4PteGlu_1$ are equally effective at inhibiting the growth of cancer cell lines *in vitro* and tumors *in vivo*.[9,10] The finding that the antiproliferative effect of $DDAH_4PteGlu_1$ is due to inhibition of GARFT sparked much interest in this compound as a drug candidate.[4,8] In contrast, two well known antifolates, aminopterin and methotrexate, both act by inhibition of dihydrofolate reductase (DHFR, EC 1.5.1.3).

Early work with $DDAH_4PteGlu_1$ indicated that cells treated with (6*R*)-$DDAH_4PteGlu_1$ rapidly convert the drug to its pentaglutamate and hexaglutamate metabolites.[11] Rapid conversion to polyglutamate forms has also been observed with purified hFPGS[12] and in the mouse.[13] It is an excellent substrate for purified mammalian FPGS with kinetic constants similar to the best natural substrates, 10-formyltetrahydrofolate (10-formyl-H_4PteGlu) and tetrahydrofolate (H_4PteGlu).[8,10,14,15] The (6*R*)- and (6*S*)-diastereomers of $DDAH_4PteGlu_1$ have K_M values with human FPGS of 1.7 and 1.0 μM respectively. Substrate inhibition was observed, but only by the (6*S*)-diastereomer.[10] It was also found that the poly-γ-glutamate forms are much more potent inhibitors of GARFT, with K_I values for $DDAH_4PteGlu_1$ and $DDAH_4PteGlu_5$ being 39 nM and 0.39 nM, respectively.[16] This increase in potency for the target enzyme upon polyglutamylation has been observed for many anti-folate compounds.[17] Resistance of cancer cells to $DDAH_4PteGlu_1$ has been observed to arise from a decrease in polyglutamylation.[11,18,19] These data strongly suggest that the polyglutamylated form of $DDAH_4PteGlu_1$ is responsible for its cytotoxic activity.

$DDAH_4PteGlu_1$ was first synthesized as a mixture of diastereomers about the C-6 position as reported by Taylor *et al.*[14] Since that time a number of other racemic syntheses have been reported.[20,21] Access to the individual diastereomers of $DDAH_4PteGlu_1$ was originally obtained by fractional crystallization or chiral HPLC of $DDAH_4PteGlu_1$ diethyl ester, *d*-10-camphorsulfonic acid salt, followed by careful saponification.[10,22] An asymmetric synthesis of (6*R*)-$DDAH_4PteGlu_1$, the diastereomer selected for clinical trials, has been reported.[23]

† Electronic supplementary information (ESI) available: Experimental details. See http://dx.doi.org/10.1039/b505907k

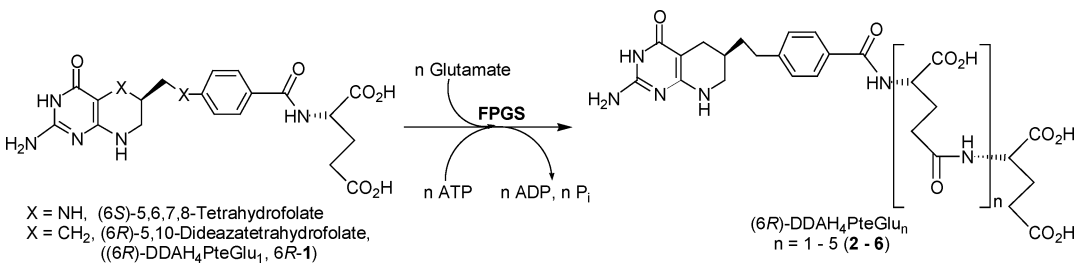

Scheme 1 The reaction of FPGS with (6*R*)-$DDAH_4PteGlu_1$ (**1**). The structure of (6*S*)-tetrahydrofolic acid is shown for comparison.

DOI: 10.1039/b505907k

In this paper, we report the syntheses of (6*R*)-$DDAH_4$PteGlu$_{1-6}$, (6*S*)-$DDAH_4$PteGlu$_{1-2}$, and (6*R*)-$DDAH_4$Pte[^{14}C]Glu$_1$ *via* a 5,10-dideaza-5,6,7,8-tetrahydropteroyl azide ($DDAH_4$Pte–N_3) intermediate that allows for the incorporation of completely unprotected L-glutamate, poly-γ-glutamate peptides, or L-[U–^{14}C]glutamate, respectively, as the final step in the synthesis.[24,25] The (6*R*)- and (6*S*)-isomers of $DDAH_4$Pte–N_3 were derived from the individual enantiomers of methyl 2-pivaloyl-5,10-dideaza-5,6,7,8-tetrahydropteroate, which, in turn, were purified from the racemic mixture[26] by chiral HPLC. The only previously reported synthesis of radiolabeled (6*R*)-$DDAH_4$PteGlu$_1$ involved a multi-step procedure in which the unstable isotope (^{3}H) was incorporated to form a racemic precursor midway through the synthesis.[27] Resolution of racemic [^{3}H]$DDAH_4$PteGlu$_1$ was required to obtain the desired single diastereomer for use in metabolic studies.[11] In contrast, in the synthesis described herein, the ^{14}C label is introduced into a single isomer, *via* (6*R*)-$DDAH_4$Pte–N_3, in the final step.

The full range of poly-γ-glutamate forms of individual folates and antifolates have been synthesized previously by both solid-phase[28–30] and solution-phase[29,31–35] chemistries. In this research, the poly-γ-glutamate peptides were synthesized by solid-phase peptide synthesis utilizing L-glutamate protected as the *N*-Fmoc and α- or γ-*tert*-butyl ester. The procedure included a capping step that prevented further elongation of any unreacted N-terminal amines. The biochemical evaluation of these compounds as substrates for hFPGS was then pursued. We report steady-state kinetics data (K_M, V_{max}, V/K) for all newly synthesized polyglutamates, and also document marked substrate inhibition by all compounds with the exception of (6*R*)-$DDAH_4$PteGlu$_1$ and (6*R*)-$DDAH_4$PteGlu$_6$.

Results and discussion

Chemistry

Synthesis of (6*RS*)-5,10-dideaza-5,6,7,8-tetrahydrofolic acid (6*RS*-**1**) was achieved *via* the route illustrated in Scheme 2. This route is based on the work of Taylor *et al.*,[26] but is modified to allow the incorporation of unprotected glutamate, radiolabeled glutamate, or poly-γ-glutamate peptides as the final synthetic step in the synthesis. This was achieved through the use of an acyl azide, **9**, derived from (6*RS*)-methyl 2-pivaloyl-5,10-dideaza-5,6,7,8-tetrahydropteroate (6*RS*-**7**). The racemic ester, 6*RS*-**7**, was separated into its individual enantiomers by chiral HPLC, enabling ready access to either the (6*R*)- or (6*S*)-isomer of $DDAH_4$PteGlu$_1$ and $DDAH_4$Pte polyglutamates.

Deprotection of **7** was achieved by basic hydrolysis in 1 M $NaOH_{aq}$. Isolation of 5,10-dideaza-5,6,7,8-tetrahydropteroic acid (**8**) involved acidification of the basic product solution with HCl to precipitate the insoluble salt, which was then collected by centrifugation. 5,10-Dideaza-5,6,7,8-tetrahydropteroyl azide (**9**) was formed by the treatment of **8** with ethyl chloroformate in the presence of triethylamine in DMSO to produce the mixed anhydride, followed by displacement with azide anion. The product was then recovered by precipitation with aqueous HCl followed by centrifugation. HPLC analysis of the reaction mixture prior to work-up consistently indicated 95–100% conversion to product. However, during the acidic aqueous workup, a significant portion of the product (5–10%) was hydrolyzed back to **8**. Since other work-up options provided no improvement in product purity and **8** would not interfere in the following steps, **9** contaminated with a small amount of **8** was carried through the subsequent transformations.

Initially, the synthesis of **9** was attempted by treating **8** with diphenylphosphoryl azide, as has been previously reported for similar antifolates.[25] Unfortunately, this reaction proceeded very slowly, with less than 50% conversion after prolonged reaction (9 days) based on HPLC analysis, in contrast to 85% conversion of 4-deoxy-4-amino-10-methylpteroic acid to the corresponding azide over a much shorter reaction time (2 days). This marked difference in reaction rate is presumably due to decreased nucleophilicity of the conjugate base of the carboxylic acid **8** (pK_a = *ca.* 4.3) *vs.* that of the corresponding pteroic acid analogue (pK_a = *ca.* 5.0).[36] Therefore, formation of a mixed anhydride followed by reaction with azide ion[37] was investigated and proved to be effective in converting **8** to **9** in nearly quantitative yield. The coupling reactions between **9** and L-glutamate or poly-γ-glutamates to produce 5,10-dideaza-5,6,7,8-tetrahydrofolic acid (**1**) or its polyglutamates (**2** through **6**) were performed in DMSO in the presence of Et_3N (*vide infra*). The optimal reaction conditions consisted of two equivalents of **9** per equivalent of amino acid or peptide with a reaction time of two days at room temperature. Any of the parent acid, **8**, formed from excess **9** due to the presence of adventitious water in the reaction mixture, or during workup, could be recovered.

The poly-γ-glutamates required for the preparation of $DDAH_4$PteGlu$_n$ were synthesized by standard solid-phase Fmoc-peptide synthesis procedures.[38] Two differently protected Fmoc-L-glutamic acid building blocks were utilized in the solid-phase synthesis. *N*-α-Fmoc-L-glutamic acid α-*tert*-butyl ester (Fmoc-Glu-(OH)O*t*-Bu) was required to obtain the desired γ-linkages, while *N*-α-Fmoc-L-glutamic acid γ-*tert*-butyl ester (Fmoc-Glu(O*t*-Bu)–OH) was used to load the *p*-benzyloxybenzyl alcohol (Wang) resin (Scheme 3). Acetic anhydride and dimethylaminopyridine (DMAP) in DMF were used in a capping step to acylate any free N-termini remaining after each peptide coupling step, thereby preventing further elongation of any unreacted peptide. Fmoc-Glu(O*t*-Bu)–OH was chosen for resin loading because it has been reported that the γ-linkage to the resin is more labile than the standard α-linkage.[28] Also, as this is the least efficient step (40–50% yield),

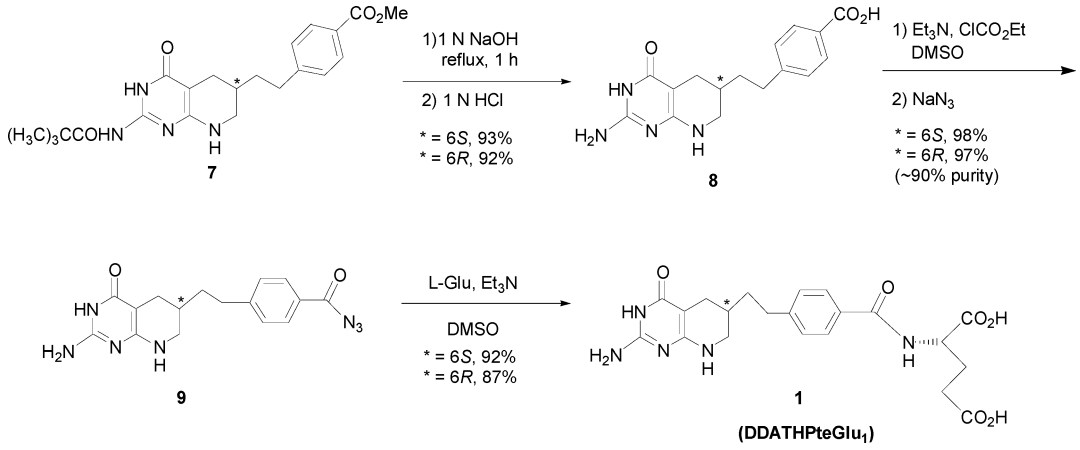

Scheme 2 Synthesis of $DDAH_4$PteGlu$_1$ (**1**) from protected $DDAH_4$Pte–OH (**7**).

Table 1 Kinetic constants of the C-6 stereoisomers of $DDAH_4PteGlu_1$

	Michaelis–Menten fit[a]		Substrate inhibition fit[b]		
	V_{max}/μM h^{-1}	K_M/μM	V_{max}/μM h^{-1}	K_M/μM	K_I/μM
6R	3.15 ± 0.11	1.93 ± 0.23	NA[c]	NA[c]	NA
6S	3.31 ± 0.15	1.06 ± 0.20	4.01 ± 0.20	1.56 ± 0.23	76 ± 10

[a] Values obtained using the Michaelis–Menten equation to fit the data in Fig. 1A. [b] Values obtained using eqn (2) to fit the (6*S*)-isomer data in Fig. 1B. [c] $K_M = 3.67 \pm 0.55$ μM and $V_{max} = 3.94 \pm 0.10$ μM h^{-1} were obtained when the Michaelis–Menten equation was used to fit the data for the (6*R*)-isomers in Fig. 1B.

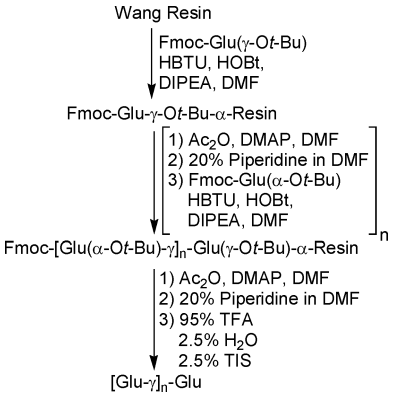

Scheme 3 Solid-phase synthesis of poly-γ-glutamate peptides.

the fact that the Fmoc-Glu(O*t*-Bu)–OH is five times less costly than Fmoc-Glu-O*t*-Bu makes its use in this reaction more attractive. This method allows for the facile synthesis of any γ-glutamyl peptide on a 100 mg scale in a few days using manual methods. Purification is achieved by reversed-phase, semi-preparative HPLC followed by lyophilization to yield the trifluoroacetate salt of the peptide. Purified γ-glutamyl peptides were coupled to 5,10-dideaza-5,6,7,8-tetrahydropteroyl azide (**9**) under the optimized conditions described above (Scheme 4).

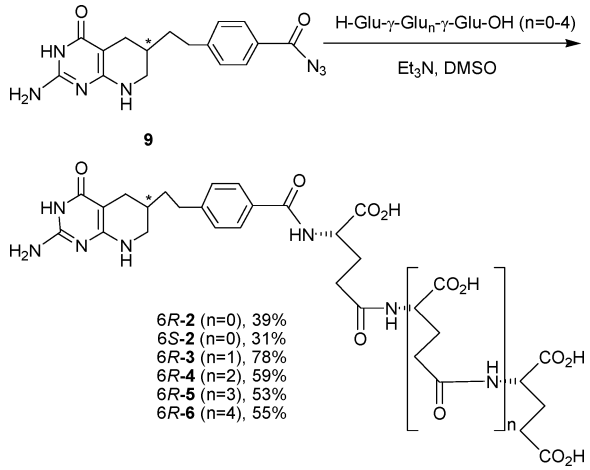

Scheme 4 Synthesis of $DDAH_4Pte$ polyglutamates (**2–6**) from $DDAH_4Pte$–N_3 (**9**). Synthesis of 6*R*-**2** and 6*S*-**2** utilized crude H-Glu-γ-Glu-OH peptide in the coupling reaction. All product yields are determined by UV/vis spectroscopy.

Biochemical studies

The biochemical studies utilized an end-point assay that quantitated the total amount of L-[^{3}H]glutamic acid ligated to the folate substrate by FPGS. Assays were performed at fixed, saturating concentrations of ATP (5 mM, *ca.* 100 × K_M) and L-glutamic acid (2 mM, *ca.* 10 × K_M) with varying concentrations of the $DDAH_4PteGlu_n$ being characterized. Both diastereomers of $DDAH_4PteGlu_1$ exhibited Michaelis–Menten kinetics at folate concentrations up to at least ~15 × K_M (Fig. 1A). The kinetic constants that were obtained (Table 1) agree with the reported values of 1.7 and 1.0 μM for the (6*R*)- and (6*S*)-diastereomers, respectively.[10]

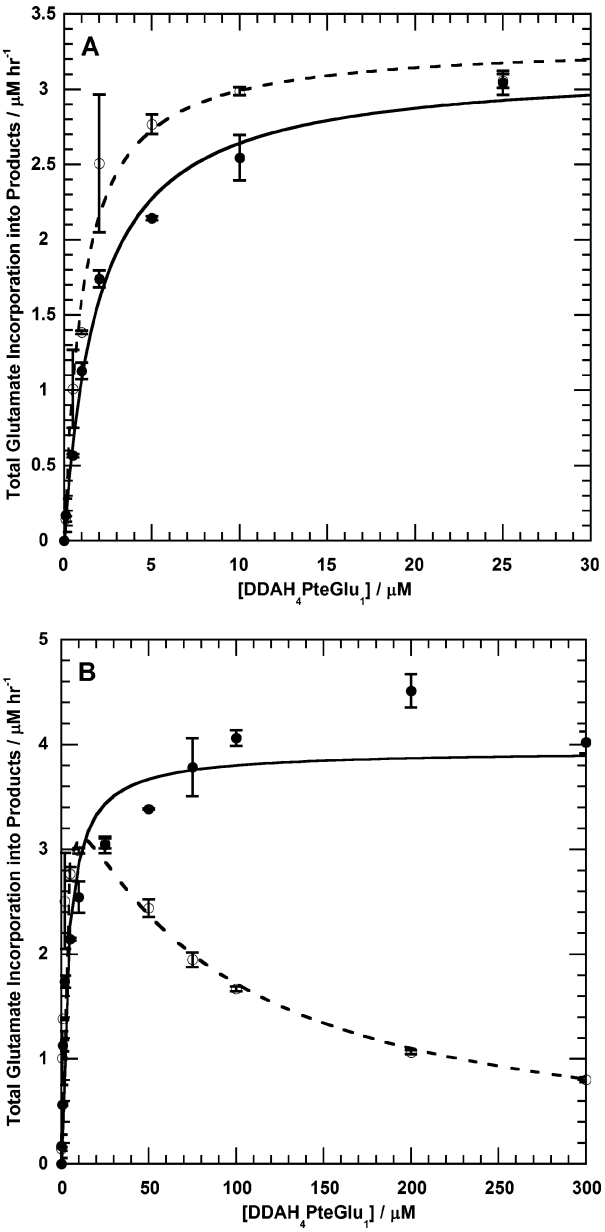

Fig. 1 Steady-state kinetics: hFPGS-catalyzed ligation of L-glutamate to each of the C-6 stereoisomers of $DDAH_4PteGlu_1$, (6*R*)- (●), and (6*S*)- (○). hFPGS was expressed in *E. coli* and partially purified. Each assay was done in duplicate and the data points shown are the average values ± range. **A**. Curves are the best fit of the data in the non-inhibitory concentration range to the Michaelis–Menten equation. **B**. Curves are the best fit of all data to the Michaelis–Menten equation (6*R*), or eqn (2) (6*S*).

However, as is apparent from Fig. 1B, the data for the (6*R*)-diastereomer at concentrations >30 μM deviate significantly from the best fit to the Michaelis–Menten equation for a single E·S complex. A model which invokes the formation of two different E·S complexes (eqn (1)) yielded a better fit to the entire range of data for the (6*R*)-diastereomer (Fig. 1B) and resulted in values of K_{M1} and K_{M2} that differed by two orders of magnitude ($K_{M1} \ll K_{M2}$, *ca.* 1 and 100 μM respectively). However, the value

$$v = \frac{V_{max}[S]}{K_{M1}+[S]} + \frac{V_{max}[S]}{K_{M2}+[S]} \quad (1)$$

of K_{M2} differs markedly from the steady state K_M value determined for the (6*R*)-$DDAH_4$Pte–Glu_2 species (*vide infra*), the presumed substrate involved in the second E·S complex. This model does not appear to be adequate to explain the deviation from Michaelis–Menten kinetics and was not pursued further.

At higher concentrations of (6*S*)-$DDAH_4PteGlu_1$ (30–300 μM), substrate inhibition was noted (Fig. 1B). This is consistent with what is known in the literature.[8,10] In order to obtain K_M, K_I, and V_{max} values from these data, a substrate inhibition equation for a simple system, eqn (2), was used.[39]

$$v = \frac{V_{max}}{1 + \frac{K_M}{[S]} + \frac{[S]}{K_I}} \quad (2)$$

It was expected that the (6*R*)- and (6*S*)-diastereomers of the poly-γ-glutamate conjugates would exhibit similar properties as was observed for the respective monoglutamate diastereomers in terms of substrate inhibition. However, as can be seen in Fig. 2, both the (6*R*)- and (6*S*)-isomers of the diglutamate, $DDAH_4PteGlu_2$, exhibit striking substrate inhibition that occurred at much lower relative concentrations (~5 × K_M) than that observed for (6*S*)-$DDAH_4PteGlu_1$. Due to the low concentration at which the substrate inhibition became significant, the Michaelis–Menten equation was used for fitting only the data in the non-inhibitory region (≤5 μM). The kinetic constants for the diastereomers of $DDAH_4PteGlu_2$ are summarized in Table 2. The observed substrate inhibition could be associated with either non-sequential kinetics and/or partial sites reactivity in an oligomeric protein. However, there is no supporting evidence for either of these scenarios for FPGS.

This substrate inhibition may be explained by two molecules of substrate binding to a single hFPGS simultaneously. The first molecule of substrate would bind in the active site correctly oriented for turnover, while the second molecule would bind to another site that inhibits catalysis. This second site could either be an allosteric binding site involved in feedback inhibition or an incorrect binding of the second folate substrate molecule in the active site. Based on the crystal structure of a binary complex (*L. casei* FPGS·ATP), the C-terminal domain of FPGS has a very similar secondary structure to that of DHFR from several species,[41] indicating a possible role in folate binding. Preliminary docking studies performed based on the crystal structure of a ternary complex (*L. casei* FPGS·AMPPCPP·5,10-CH_2-$H_4PteGlu_1$)[42] indicates the possible presence of a second folate substrate binding site on the N-terminal domain of the protein (Dr Heather Carlson, University of Michigan, personal communication). Recent work by Mathieu *et al.* supports this finding. A second folate substrate binding site with dihydropteroate bound was observed when a structure of the bifunctional *E. coli* FolC enzyme, harboring dihydrofolate synthetase and folylpolyglutamate synthetase activities, was determined.[43]

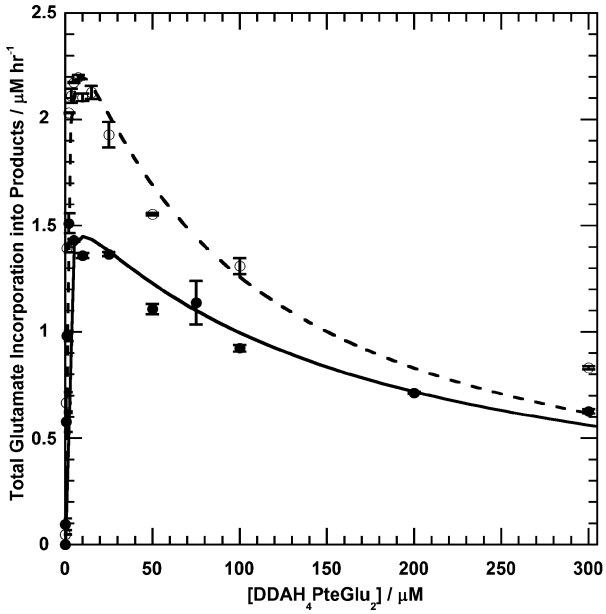

Fig. 2 Steady-state kinetics: hFPGS-catalyzed ligation of L-glutamate to each of the C-6 stereoisomers of $DDAH_4PteGlu_2$, (6*R*)- (●), and (6*S*)- (○). hFPGS was expressed in *E. coli* and partially purified. Each assay was done in duplicate and the data points shown are the average values ± range. Curves shown are the best fit of all data to eqn (2). Data in the non-inhibitory range were fit to the Michaelis–Menten equation.

The trend of substrate inhibition carried through the entire series of (6*R*)-$DDAH_4PteGlu_n$ (n = 3–5, Fig. 3). Of the polyglutamate compounds, only the hexaglutamate exhibited Michaelis–Menten behaviour. Table 3 lists the kinetic constants obtained from the (6*R*)-$DDAH_4PteGlu_n$ compounds.[44] As glutamate chain-length increased (n = 1–5), the V/K values first increased approximately 2.5-fold when going from the mono- to diglutamate species. This difference arises from a much lower K_M value for the latter. The tri-, tetra-, and pentaglutamates exhibited much lower, but similar, V/K values than those observed for the shorter chain length substrates due to much reduced V_{max} values. These data follow the same general pattern reported by Chen *et al.* for pteroyl and (6*S*)-tetrahydropteroyl poly-γ-glutamate$_n$ (n = 1–5).[45] A similar trend has been reported for FPGS from *L. casei*, an enzyme for which a crystal structure is available.[42] Analysis of this structure indicates that the γ-carboxyl group of the monoglutamate substrate does not reach the ATP and is therefore incapable of forming the γ-glutamyl phosphate[46] without significant, and energetically costly, conformational changes. However, the diglutamate is perfectly accommodated in the active site.[47] There is no indication of how longer chain length products could be accommodated within the active site. In the current work, a very low value of V/K

Table 2 Kinetic constants of the C-6 stereoisomers of $DDAH_4PteGlu_2$

	Michaelis–Menten fit[a]		Substrate inhibition fit[b]		
	V_{max}/μM h^{-1}	K_M/μM	V_{max}/μM h^{-1}	K_M/μM	K_I/μM
6R	1.84 ± 0.24	0.87 ± 0.33	1.64 ± 0.11	0.65 ± 0.17	157 ± 25
6S	2.83 ± 0.29	1.16 ± 0.35	2.65 ± 0.15	0.95 ± 0.20	92 ± 20

[a] Values obtained using the Michaelis–Menten equation to analyze the data in the non-inhibitory region (≤5 μM). Similar values were obtained when the data were analyzed utilizing the Hanes linear transform.[40] [b] Values obtained using eqn (2).

Table 3 Kinetic constants of (6*R*)-DDAH$_4$PteGlu$_n$[a]

n	V_{max}/μM h^{-1}	K_M/μM	K_I/μM	(V/K)/h^{-1}
1	3.94 ± 0.10	3.67 ± 0.55	NA	1.07 ± 0.16
2	1.64 ± 0.08	0.65 ± 0.12	157 ± 25	2.52 ± 0.48
3	0.30 ± 0.03	0.96 ± 0.43	179 ± 91	0.31 ± 0.14
4	0.71 ± 0.07	1.60 ± 0.55	144 ± 56	0.44 ± 0.16
5	0.22 ± 0.01	1.05 ± 0.24	417 ± 152	0.21 ± 0.05
6	0.59 ± 0.02	14.5 ± 1.9	NA	0.04 ± 0.01

[a] Values obtained using the Michaelis–Menten equation ($n = 1$ and 6) or eqn (2) ($n = 2$–5).

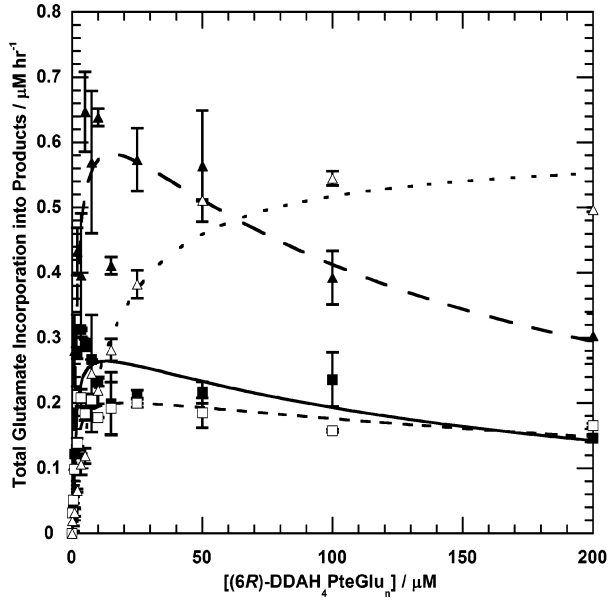

Fig. 3 Steady-state kinetics: hFPGS-catalyzed ligation of L-glutamate to (6*R*)-DDAH$_4$PteGlu$_n$ (n = 3–6). hFPGS was expressed in bacculovirus-infected SF9 insect cells and partially purified. Each assay was done in duplicate and the data points shown are the average values ± range. $n = 3$ (■), 4 (▲), 5 (□), and 6 (△). Curves are the best fit of all data to the Michaelis–Menten equation ($n = 6$) or eqn (2) ($n = 3$–5).

for (6*R*)-DDAH$_4$PteGlu$_6$ was determined, due primarily to a significantly increased value of K_M.

One caveat in these analyses is that multiple glutamate ligations are occurring during the reactions, *i.e.*, the di-, tri-, tetra-, *etc.* glutamate products are formed since each product is also a substrate for further ligation. This complexity makes the following assumptions in the standard Michaelis–Menten analysis invalid: (1) only a single substrate and single enzyme–substrate complex are involved, (2) the enzyme–substrate complex breaks down directly to form free enzyme and product, and (3) enzyme, substrate, and enzyme–substrate complex are at equilibrium, *i.e.*, the dissociation of ES to E + S is rapid in comparison to the formation of E + P.[48]

To establish that multiple glutamate ligations were occurring to a single folate substrate, product distribution analysis was done at varied (6*R*)-DDAH$_4$Pte[^{14}C]Glu$_1$ concentrations. When these reactions were analyzed, it was determined that multiple products were produced and that the product distribution varied with changing concentrations of (6*R*)-DDAH$_4$PteGlu$_1$ (Fig. 4). The observed trend is that progressively shorter chain length products are produced with increasing concentrations of (6*R*)-DDAH$_4$PteGlu$_1$. The results of this experiment are very similar to those observed for rat liver FPGS with (6*RS*)-H$_4$PteGlu as the substrate.[49] In that case, multiple glutamate ligations to (6*RS*)-H$_4$PteGlu at 5 μM ($\sim K_M$) yielded H$_4$PteGlu$_{4-5}$ as the predominant products, following initial formation of H$_4$PteGlu$_2$ and H$_4$PteGlu$_3$ that built up to a low level and subsequently

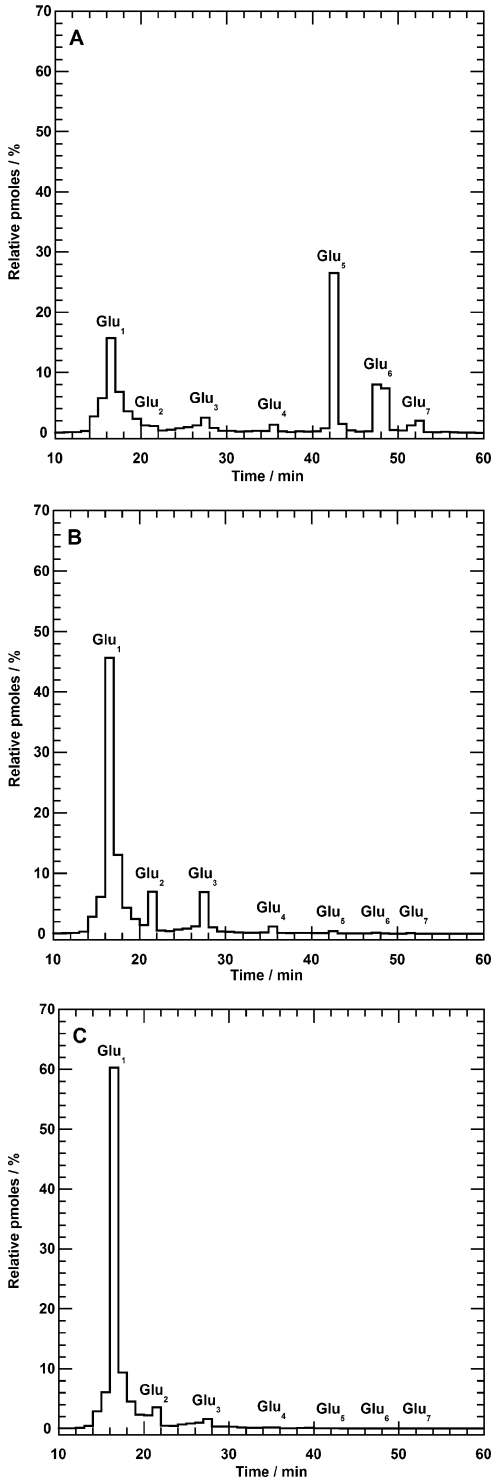

Fig. 4 Product distribution of reactions of (6*R*)-DDAH$_4$Pte[^{14}C]Glu$_1$ with purified hFPGS expressed in bacculovirus-infected SF9 insect cells. The concentrations of the glutamate and ATP substrates were 5 mM and 10 mM respectively. Reactions contained the following concentrations of (6*R*)-DDAH$_4$Pte[^{14}C]Glu$_1$: **A**. 2.5 μM. **B**. 25 μM. **C**. 250 μM.

decreased. In contrast, (6*RS*)-H$_4$PteGlu at 35 μM ($\sim 10 \times K_M$) yielded predominately H$_4$PteGlu$_2$ and H$_4$PteGlu$_3$; H$_4$PteGlu$_{4-5}$ products were only observed at longer reaction times.

The product distribution results at a low concentration, 2.5 μM, agree well with what has been observed in whole CCRF-CEM cells[11] and in the livers of mice[13] that were treated with (6*R*)-DDAH$_4$PteGlu$_1$. In cells treated with 10 μM (6*R*)-DDAH$_4$PteGlu$_1$, polyglutamate products (n = 2–6) were observed even at the earliest time point, 4 h, with the pentaglutamate product predominating at longer incubation times.

Analysis of the livers of mice dosed with 0.72 mg kg^{-1} of (6*R*)-$DDAH_4PteGlu_1$ indicated that the pentaglutamate product was formed relatively quickly with no detectable diglutamate product and smaller amounts of tri-, tetra- and hexaglutamate products.

In an attempt to explain these product distributions, a kinetic modeling study was undertaken. This study utilized the K_M and V_{max} values listed in Table 3 and a minimum mechanism based on sequential elongation of the substrate. Product release between each catalytic step was assumed, *i.e.*, a distributive mechanism, so that the Michaelis–Menten kinetic equation could be utilized to analyze these data. Substrate inhibition by the polyglutamates was ignored because of the low concentrations of products formed in the reactions. Modeling of this distributive mechanism, while able to produce different product distributions with differing initial monoglutamate substrate concentrations, was unable to mimic the product distributions actually observed. A model in which product release was not mandated between each catalytic step, *i.e.* a processive mechanism, could not be readily developed. However, a processive mechanism was assessed directly by subsequent substrate-trapping and pulse-chase experiments, the results of which will be published separately.

Conclusions

In this paper, we report the synthesis of the antifolate drug Lometrexol™ ((6*R*)-$DDAH_4PteGlu_1$), its poly-γ-glutamates ((6*R*)-$DDAH_4PteGlu_{2-6}$), and a radiolabeled form ((6*R*)-$DDAH_4Pte[^{14}C]Glu_1$). In addition, the (6*S*)-isomers, (6*S*)-$DDAH_4PteGlu_1$ and (6*S*)-$DDAH_4PteGlu_2$, were synthesized. To obtain the single isomer materials, a chiral HPLC separation of (6*RS*)-methyl 2-pivaloyl-5,10-dideazatetrahydropteroate (6*RS*-**7**) was developed. This separation was achieved on a preparative scale (~5 g) and resulted in material with an isomeric purity of >98%. The isomerically pure materials were subsequently used in the preparation of all $DDAH_4PteGlu_n$ compounds as well as (6*R*)-$DDAH_4Pte[^{14}C]Glu_1$. These compounds were then evaluated as substrates for recombinant human cytosolic FPGS, and the kinetic data augmented by reaction product analysis.

The observed biochemical properties of the (6*R*)- and (6*S*)-diastereomers of $DDAH_4PteGlu_1$, including the segregation of substrate inhibition to the (6*S*)-diastereomer, are comparable to that previously reported in the literature. The properties of the single diastereomers of $DDAH_4PteGlu_2$ are reported for the first time and show no such separation of the substrate inhibition. Indeed, all of the (6*R*)-$DDAH_4PteGlu_{2-5}$ compounds show substrate inhibition. (6*R*)-$DDAH_4PteGlu_6$ is the only polyglutamate substrate not to exhibit substrate inhibition.

When the kinetic constants for the (6*R*)-$DDAH_4PteGlu_n$ compounds are compared (Table 3), it is seen that the diglutamate has the highest V/K value. The value for the diglutamate is over two-fold greater than that obtained for monoglutamate indicating that the diglutamate is the preferred substrate for hFPGS. This is primarily due to the much lower K_M for the diglutamate *vs.* the monoglutamate which overcomes the lower V_{max} of the former. The rest of the poly-γ-glutamates, tri- through hexaglutamate, exhibit V/K values of less than half that of the monoglutamate, indicating that they are much poorer substrates than the mono- and diglutamate compounds.

It is also apparent that the product distributions obtained utilizing (6*R*)-$DDAH_4Pte[^{14}C]Glu_1$ exhibit a significant dependence on substrate concentration (Fig. 4). The experimentally observed product distributions are similar to those observed in cells and whole animals. This similarity of product distributions (*in vitro vs. in vivo*) provides strong support for the validity of applying conclusions obtained from this work to what may be occurring *in vivo*.

Experimental

Materials

Common solvents and reagents were obtained from commercial sources and were of the highest purity available. L-[2,3-^{3}H]-Glutamic acid (NET-395) and L-[U-^{14}C]glutamic acid (NEC-290E) were obtained from Perkin–Elmer Life Sciences. *p*-Benzyloxybenzyl alcohol (Wang) resin, *N*-α-Fmoc-L-glutamic acid α-*tert*-butyl ester (Fmoc-Glu(OH)–O*t*-Bu), *N*-α-Fmoc-L-glutamic acid γ-*tert*-butyl ester (Fmoc-Glu(O*t*-Bu)–OH), *N*-hydroxybenzotriazole–H_2O (HOBt), benzotriazole-1-yloxytris-(pyrrolidino)phosphonium hexafluorophosphate (PyBOP), and 2-(1*H*-benzotriazole-1-yl)-1,1,3,3-tetramethyluronium hexafluorophosphate (HBTU) utilized for solid phase peptide synthesis were obtained from NovaBiochem. $CDCl_3$, D_2O, d-TFA, and NaOD were from Isotec and d_6-DMSO was from Cambridge. (6*R*)-5,10-Dideaza-5,6,7,8-tetrahydrofolic acid sodium ((6*R*)-$DDAH_4PteGlu_1$–Na, Lometrexol™ sodium, Lot 235MH8) and (6*RS*)-5,10-dideaza-5,6,7,8-tetrahydropteroyl polyγ-glutamates ($DDAH_4PteGlu_2$, Lot 266251 and $DDAH_4PteGlu_5$, Lot 266578) were kind gifts of Dr Chuan Shih, Eli Lilly & Co, Indianapolis, IN. These compounds were used only in initial studies on assay development and for comparison of physical properties with newly synthesized compounds. (6*RS*)-Methyl 2-pivaloyl-5,10-dideazatetrahydropteroate (6*RS*-**7**) was synthesized as described by Taylor[26] with significant procedural modifications. Details may be found in the Supplementary Information. Spin-X HPLC 0.2 μm nylon microcentrifuge filters (spin filters) were obtained from Costar. Human folylpolyglutamate synthetase was expressed in *E. coli* or bacculovirus-infected SF9 insect cells[12,45] and partially purified as described previously.[50] Homogenous hFPGS, expressed in bacculovirus-infected SF9 insect cells and purified as described previously,[12] was a generous gift of Dr Richard Moran. hFPGS concentration was determined by the method of Bradford[51] corrected for protein purity as determined by quantitative PAGE.

General procedures

All synthetic reactions were carried out in oven-dried glassware. Moisture-sensitive reactions were carried out under a dry atmosphere of nitrogen or argon. Solvents and liquid reagents were measured and dispensed in oven-dried glass syringes or dry nitrogen-flushed disposable syringes with oven-dried needles. Et_3N, pyridine, MeOH, and CH_3CN were distilled from CaH_2. THF was distilled from benzophenone and sodium. ^{1}H and ^{13}C NMR spectra were recorded on a Bruker 300 or 500 MHz instrument using either TMS or solvent peaks as an internal reference. When an internal reference was not available (*e.g.* a ^{13}C NMR spectrum in D_2O) the frequency of the solvent deuterium was utilized. ^{1}H NMR assignments of diastereotopic protons are noted as, *e.g.* "1.86 (1 H, m, $C(8)H_2$), 2.07 (1 H, m, $C(8)H_2$)" and signify that each of the two methylene protons attached to carbon 8 have unique chemical shifts of 1.86 and 2.07. All chemical shifts (δ) are reported in ppm. Assignments for nuclei in the γ-glutamyl peptide portion use the prime notation (*e.g.*, C(9′)) to distinguish them from nuclei in the didezatetrahydropteroyl portion (Supplementary Information, Schemes S2 and S3). Assignment of peaks as indicated was aided and confirmed by the acquisition of various 2D spectra (COSY, HETCOR, COLOC). Nominal and high resolution mass spectra utilizing electrospray ionization with positive detection utilized Na^+ and/or H^+ matrices. Nominal mass spectral data are reported only for those fragments with a relative intensity of ≥20% of the base peak. UV/visible spectra were recorded on a Beckman Model 640B spectrophotometer. Melting points were determined with a MEL-TEMP apparatus and are reported uncorrected. Scintillation counting was carried out with a Packard 1600 scintillation counter using Bio-Safe II

scintillation cocktail from Research Products Inc. and 20 mL glass scintillation vials with foil-lined lids or 5.5 mL polypropylene multi vials from Life Science Products. The analytical HPLC system used was manufactured by Varian and consisted of a Model 410 auto-sampler, two Model 210 Prostar pumps, a Model 330 photo diode array detector, and a Model 701 fraction collector. The semi-preparative HPLC system was manufactured by Rainin and consisted of two Rabbit Model HPX pumps fitted with 50 mL min^{-1} pump heads, a dynamic mixer, and a single wavelength UV detector. Varian Star v6.3 software controlled both systems. All HPLC was run at ambient temperature. Optical rotation was determined with a Perkin–Elmer Model 241 polarimeter using the sodium D line source (589 nm) with an integration time of 5 s, at ambient temperature, a cell length of 10.002 cm, and with a solution concentration of 10 mg mL^{-1} unless otherwise noted. $[\alpha]_D$ values are given in 10^{-1} deg cm^2 g^{-1} and are uncorrected. All kinetics data were fitted using KaleidaGraph v3.5, Synergy Software (Reading, PA).

Chromatography methods

Size-exclusion chromatography. A 1.6 × 80 cm column was packed with Bio-Gel P-2 (Bio-Rad, fine mesh) that had been previously swelled and equilibrated with aqueous 50 mM ammonium bicarbonate, pH 8.1. Flow through the column was gravity controlled with a 10 cm column head whose level was maintained with a siphoning system. Fractions (150-drop, ~3.4 mL) of column eluant were collected beginning with column loading. Elution of products was monitored by UV/visible absorbance, scintillation counting, and/or ninhydrin staining.

Semi-preparative reversed-phase (RP)–HPLC. All separations utilized a Varian Dynamax 21.4 × 250 mm, Microsorb 60–8, C18 column with a flow rate of 21 mL min^{-1}. Methods 1–4 utilized Eluant A consisting of 0.1% w/v TFA in ddH_2O, pH 1.8. Eluant B consisting of 0.1% w/v TFA in CH_3CN, and detection at 214 nm with gradient profiles as follows:

Method 1: 0 min, 1% B; 2 min, 1% B; 15 min, 10% B.

Method 2: 0 min, 1% B; 5 min, 1% B; 15 min, 10% B; 20 min, 100% B.

Method 3: 0 min, 5% B; 5 min, 5% B; 20 min, 15% B; 25 min, 50% B.

Method 4: 0 min, 2% B; 2 min, 2% B; 20 min, 15% B; 25 min, 50% B.

Methods 5–8 utilized an Eluant A consisting of 20 mM ammonium acetate, pH 6.5, in ddH_2O, an Eluant B consisting of MeOH, and detection at 280 nm with gradient profiles as follows:

Method 5: 0 min, 5% B; 25 min, 20% B; 30 min, 50% B; 35 min, 50% B.

Method 6: 0 min, 2% B; 25 min, 20% B; 30 min, 50% B; 35 min, 50% B.

Method 7: 0 min, 2% B; 2 min, 2% B; 25 min, 15% B; 30 min, 50% B; 35 min, 50% B.

Method 8: 0 min, 2% B; 2 min, 2% B; 25 min, 10% B; 30 min, 50% B; 35 min, 50% B.

Analytical RP-HPLC. Method 1:[24] Eluant A: 50 mM sodium phosphate buffer, pH 7.0. Eluant B: CH_3CN. Column: Chrompack Kromasil 100 Å, C18, 4.6 × 250 mm. Flow rate: 0.7 mL min^{-1}. Gradient: 0 min, 2% B; 25 min, 50% B; 35 min, 50%B. Monitored at 280 nm or scintillation counting of 30 s fractions.

Method 2: Eluant A: 0.1% w/v TFA in ddH_2O, pH 1.8. Eluant B: 0.1% w/v TFA in CH_3CN. Column: Vydac 218TP54, 5 µm, C18 protein and peptide, 4.6 × 250 mm. Flow rate: 1.0 mL min^{-1}. Isocratic at 13% B. Monitored at 280 nm.

Method 3: Eluant A: ddH_2O. Eluant B: CH_3CN. Column: Vydac 218TP54, 5 µm, C18 protein and peptide, 4.6 × 250 mm. Flow rate: 1.0 mL min^{-1}. Gradient: 0 min, 30% B; 1 min, 30% B; 20 min, 60% B; 25 min, 100% B; 40 min, 100% B. Monitored at 280 nm.

Ion-pair HPLC. Eluant A: 100% ddH_2O. Eluant B: 65% CH_3CN, 35% ddH_2O. Both eluants A and B contain 1 mM KH_2PO_4, 5 mM tetrabutylammonium phosphate (TBAP), 7 mM NaCl, and 3 mM NaN_3. Column: Vydac 218TP54, 5 µm, C18 protein and peptide, 4.6 × 250 mm. Flow rate: 1.0 mL min^{-1}. Gradient: 0 min, 10% B; 5 min, 10% B; 10 min, 36% B; 20 min, 40% B; 50 min, 55% B; 53 min, 100% B, 58 min, 100% B. Monitored at 280 nm or by the scintillation counting of fractions. This method was developed from a previously published procedure.[52]

Ion-pairing buffers for HPLC were prepared as follows. 1 L of a 10 × stock solution was prepared and consisted of 10 mM KH_2PO_4, 50 mM TBAP, 70 mM NaCl, and 30 mM NaN_3 in ddH_2O. For both eluants A and B, 100 mL of the 10 × stock solution was measured using a graduated cylinder and added to a 1 L volumetric flask. The graduated cylinder was rinsed two times with 100 mL ddH_2O and once with 50 mL ddH_2O. The eluants A and B were brought up to 1 L with ddH_2O and CH_3CN respectively and filtered through a 0.2 µm nylon filter.

Equilibration of the HPLC column was achieved in two steps. The first step was preparation of the column for the ion-pairing buffers and consists of washing the column at 1 mL min^{-1} with ddH_2O (A) and CH_3CN (B). Gradient: 0 min, 100% B; 5 min, 100% B; 8 min, 50% B; 10 min, 50% B. The flow was stopped and the pumps were switched to ion-pair containing eluants A and B. The flow was resumed at 1 mL min^{-1} and 100% B until the operating pressure had been reached. Gradient: 0 min, 100% B; 10 min, 100% B; 15 min, 10% B; 30 min, 10% B.

Chiral-HPLC (analytical). Eluant A: ddH_2O. Eluant B: CH_3CN. Column: Chiral Technologies (DAICEL Chemical Industries, LTD) Chiralcel OJ–R, 4.6 × 150 mm. Isocratic at 40% B. Flow rate: 0.5 mL min^{-1}. Monitored at 280 nm.

Chiral-HPLC (preparative). Eluant A: hexane. Eluant B: EtOH. Column: Chiralcel OJ, 2 cm × 25 cm. Isocratic at 70% B. Flow rate: 30 mL min^{-1}. Run time: 22 min. Sample concentration: 1.25 mg mL^{-1} in 25% A: 75% B. Monitored at 240 nm.

(6*R*)- and (6*S*)-Methyl 2-pivaloyl-5,10-dideaza-5,6,7,8-tetrahydropteroate (6*R*-7 and 6*S*-7). (6*RS*)-Methyl 2-pivaloyl-5,10-dideaza-5,6,7,8-tetrahydropteroate (6*RS*-**7**, 4.75 g) was resolved into its individual isomers by preparative chiral-HPLC as described above (see Supplementary Information, Figure S1). This separation was done at the Analytical Development Department, Pfizer Global Research and Development, Ann Arbor, MI. The (6*R*)-isomer (6*R*-**7**) (1.6 g) was obtained in 98.2% chiral purity (t_r = 15.2 min) as determined by analytical chiral HPLC (see Supplementary Information, Figure S2). $[\alpha]_D$ = −44.5 (MeOH–$CHCl_3$ 1.5 : 98.5); *m/z* (ESI^+) 435.2020 ($M + Na^+$. $C_{22}H_{28}N_4NaO_4$ requires 435.2008) 436 (25%), and 435 (100). The (6*S*)-isomer (6*S*-**7**) (1.8 g) was obtained in 98.2% chiral purity (t_r = 10.6 min) as determined by analytical chiral HPLC (see Supplementary Information, Figure S2). $[\alpha]_D$ = +39.7 (MeOH–$CHCl_3$ 1.5 : 98.5); *m/z* (ESI^+) 435.2015 ($M + Na^+$. $C_{22}H_{28}N_4NaO_4$ requires 435.2008) 436(25%), and 435(100). It is noted that the optical rotations of the isomers are not equal and opposite but chiral HPLC analysis provides strong evidence of extremely high stereochemical purity of both diastereomers.

(6*R*)-5,10-Dideaza-5,6,7,8-tetrahydropteroic acid (6*R*-8). (6*R*)-2-Pivaloyl-5,10-dideaza-5,6,7,8-tetrahydropteroic acid methyl ester (6*R*-**7**) (250 mg, 0.242 mmol) was suspended in 6.1 mL 1 M NaOH. A reflux condenser was fitted to the flask and the reaction was heated at reflux temperature for 30 min after the starting material had completely dissolved. The flask was then cooled to ambient temperature, and the solution was filtered through a paper filter, which was then

washed with water. The pH of the filtrate was adjusted to ~1 with 6.7 mL of 1 M HCl. The resulting suspension was lyophilized to a small volume and resuspended in water for centrifugation. The precipitate was collected by centrifugation (15 min, 4 °C, 12 000*g*) to obtain the desired product as a pellet. The pellet was then washed with ddH_2O (2 × 10 mL), CH_3CN (2 × 10 mL), and Et_2O (1 × 10 mL). The product was dried under high vacuum in the presence of P_2O_5. Ion-pair HPLC indicated >99% product purity. (196 mg, 92%); $[\alpha]_D$ = −49.5 (0.1 M NaOH) (lit.,[23] $[\alpha]_D$ = −48.3 (1 N NaOH, from the acid hydrolysis of (6*R*)-DDAH$_4$PteGlu$_1$) and $[\alpha]_D$ = −52.6 (1 N NaOH)); δ_H (300 MHz; 0.1 M NaOD in D_2O) 1.60 (2 H, m, C(10)H_2), 1.73 (1 H, m, C(6)H), 1.97 (1 H, dd, J = 8.8, 15.5 Hz, C(5)H_2), 2.53 (1 H, m, C(9)H_2), 2.72 (2 H, m, C(5)H_2 and C(9)H_2), 2.85 (1 H, m, C(7)H_2), 3.23 (1 H, m, C(7)H_2), 7.30 (2 H, d, J = 8.1 Hz, C(12)H and C(16)H), 7.74 (2 H, d, J = 8.1 Hz, C(13)H and C(15)H); m/z (ESI$^+$) 315.1448 (M + H$^+$. $C_{16}H_{19}N_4O_3$ requires 315.1457) 316(23%), 315(100), and 274(28); Ion-pair HPLC, t_r = 15.8 min. Spectral data are identical to those reported for this compound in the literature.[23]

(6*S*)-5,10-Dideaza-5,6,7,8-tetrahydropteroic acid (6*S*-8). (6*S*)-2-Pivaloyl-5,10-dideaza-5,6,7,8-tetrahydropteroic acid methyl ester (6*S*-**7**) was used in a procedure identical to that described for the synthesis of (6*R*)-5,10-dideaza-5,6,7,8-tetrahydropteroic acid (6*R*-**8**). Ion-pair HPLC indicated >99% product purity. (197 mg, 93%); $[\alpha]_D$ = +44.5 (0.1 M NaOH) (lit.,[53,54] $[\alpha]_D$ = +40.7 (1 N NaOH) and $[\alpha]_D$ = +48.3 (1 N NaOH, from the acid hydrolysis of (6*S*)-DDAH$_4$PteGlu$_1$)); δ_H (300 MHz; 0.1 M NaOD in D_2O) 1.59 (2 H, m, C(10)H_2), 1.73 (1 H, m, C(6)H), 1.96 (1 H, dd, J = 8.8, 15.5 Hz, C(5)H_2), 2.52 (1 H, m, C(9)H_2), 2.71 (2 H, m, C(5)H_2 and C(9)H_2), 2.85 (1 H, m, C(7)H_2), 3.23 (1 H, m, C(7)H_2), 7.29 (2 H, d, J = 8.1 Hz, C(12)H and C(16)H), 7.73 (2 H, d, J = 8.1 Hz, C(13)H and C(15)H); m/z (ESI$^+$) 315.1456 (M + H$^+$. $C_{16}H_{19}N_4O_3$ requires 315.1457) 316(24%), 315(94), 305(48), 297(21), 275(24), 274(100), 268(50), 233(31), and 79(40); Ion-pair HPLC, t_r = 15.9 min.

(6*R*)-5,10-Dideaza-5,6,7,8-tetrahydropteroyl azide (6*R*-9). (6*R*)-5,10-Dideaza-5,6,7,8-tetrahydropteroic acid (6*R*-**8**) (47 mg, 0.13 mmol) was added under Ar to a dry flask containing a stir bar. The flask was sealed with a septum under an atmosphere of Ar (balloon) before the addition of 1 mL anhydrous DMSO. The solution was cooled in a 20 °C water bath before the addition of Et_3N (107 μL, 0.77 mmol). After 15 min, cold ethyl chloroformate (14 μL, 0.15 mmol) was added. After 45 min, NaN_3 (10.5 mg, 0.16 mmol) was then added. The reaction was allowed to stir for 1 h at ambient temperature. Reaction completion was verified by RP-HPLC, Method 1. The reaction solution was diluted with 6 mL of 0.1 M HCl for precipitation. The precipitate was collected by centrifugation (15 min, 4 °C, 12 000*g*). The supernatant was removed and the pellet was washed with: 1 × 10 mL ddH_2O; 1 × 10 mL CH_3CN; and 1 × 5 mL Et_2O. The pellet was allowed to air-dry for 15 min before drying under high vacuum in the presence of P_2O_5 for several hours. Total mass recovery, 49 mg, a mixture of 6*R*-**9** (90.5%) and 6*R*-**8** based on RP-HPLC (Method 1); Ion-pair HPLC, t_r = 30.6 min. This material was used in subsequent coupling reactions without further purification. Because of concerns about stability, ^{1}H NMR spectra were not obtained. These data for racemic **9** are reported in the Supplementary Information.

(6*S*)-5,10-Dideaza-5,6,7,8-tetrahydropteroyl azide (6*S*-9). (6*S*)-5,10-Dideaza-5,6,7,8-tetrahydropteroic acid (6*S*-**8**) was used in a procedure identical to that described for the synthesis of (6*R*)-5,10-dideaza-5,6,7,8-tetrahydropteroyl azide (6*R*-**9**). Total mass recovery, 51 mg, a mixture of 6*S*-**9** (89.6%) and 6*S*-**8** based on RP-HPLC (Method 1); Ion-pair HPLC, t_r = 30.4 min. This material was used in subsequent coupling reactions without further purification. Because of concerns about stability, ^{1}H NMR spectra were not obtained. These data for racemic **9** are reported in the Supplementary Information.

Solid phase synthesis of glutamyl-γ-glutamate peptides (H-Glu-γ-Glu$_n$-γ-Glu-OH, n = 0–4). Typical procedure.[38] L-Glutamyl-γ-L-glutamate (γ-Glu$_2$).

Resin loading. .714 g (4.03 mmol) Fmoc-Glu(O*t*-Bu)–OH, 0.545 g (4.03 mmol) HOBt, and 2.06 g (3.95 mmol) PyBOP were dissolved in 10 mL of anhydrous DMF in a dry test tube with gentle mixing. After 15 min, 1.5 mL (8.64 mmol) of DIPEA was added to the test tube with gentle mixing. After 5 min, this solution was added to a reaction tube containing 0.905 g (1.08 mmol) of swelled Wang resin. After 90 min of agitation by inversion at ambient temperature, the reaction was stopped by filtering the resin and washing with 3 × 10 mL DMF and 2 × 10 mL CH_2Cl_2. Loading yield was determined by Fmoc quantification as follows. Two samples of loaded resin (approximately 1 mg each) were accurately weighed out and placed in two test tubes. A third tube lacking resin was used as the blank. 3 mL of 20% piperidine in DMF was added to each tube with agitation for 3 min. The solutions were then placed in quartz cuvettes and their absorbance at 290 nm measured. After subtracting the blank absorbance, eqn (3)[38] was used to determine that a loading yield of 0.53 mmol g^{-1} (44%) was achieved.

$$\text{mmol g}^{-1} = \frac{\text{OD}_{290}}{\text{mg resin} \times 1.65} \quad (3)$$

Capping. A solution of 0.20 mL (2.16 mmol) acetic anhydride and 0.132 g (1.08 mmol) DMAP in 10 mL of anhydrous DMF was added to the resin. The mixture was agitated by inversion for 60 min at ambient temperature. The reaction was stopped by filtering the resin and washing with 3 × 10 mL DMF and 2 × 10 mL CH_2Cl_2.

Deprotection. 50 mL of a 20% (v/v) solution of piperidine in anhydrous DMF was prepared. 10 mL of this solution was added to the resin with agitation. After 3 min, the resin was filtered and the above deprotection steps were repeated four times. After the final filtration, the resin was washed with 3 × 10 mL DMF and 2 × 10 mL CH_2Cl_2.

Coupling. 0.808 g (1.90 mmol) Fmoc-Glu-O*t*-Bu, 0.257 g (1.90 mmol) HOBt, and 0.702 g (1.85 mmol) HBTU were dissolved in 10 mL of anhydrous DMF in a dry test tube with gentle mixing. After 15 min, 0.66 mL (3.80 mmol) of DIPEA was added to the test tube with gentle mixing. After 5 min, this solution was added to a reaction tube containing the resin to which the C-terminal Glu$_n$ was attached. After 90 min of agitation by inversion at ambient temperature, the reaction was stopped by filtering the resin and washing with 3 × 10 mL DMF and 2 × 10 mL CH_2Cl_2.

Capping and deprotection. As above.

Cleavage/deprotection. The resin was transferred to a 25 mL round-bottomed flask and mixed with 9.5 mL TFA, 2.5 mL ddH_2O, and 2.5 mL TIS. After 90 min at ambient temperature with occasional swirling, the solution was filtered and the resin was washed with TFA. The combined filtrates were concentrated *in vacuo*. The residue was then diluted with ddH_2O and lyophilized to remove trace TFA. The residue was dissolved in ddH_2O with the resulting solution being filtered with a 0.2 μm PTFE syringe filter prior to lyophilization. Mass spectral analysis indicated the presence of a significant amount of the mono-*tert*-butyl ester so the deprotection step was repeated as above except utilizing 9.5 mL TFA, 0.25 mL ddH_2O, and 0.25 mL TIS. Lyophilization yielded the crude dipeptide (172 mg, 93%). A portion of this material, 154 mg, was then purified by semi-preparative RP-HPLC (Method 1), t_r = 6.4 min, to obtain the TFA salt of the dipeptide after lyophilization. Total yield 75 mg (40% based on total resin loading, 45% based on fraction of crude material purified). δ_H (500 MHz; D_2O; numbering system for Glu$_{2-6}$, see Supplementary Information Scheme S2) 1.96 (1 H, m, C(8′)H_2), 2.14 (3 H, m, C(3′)H_2 and C(8′)H_2), 2.46 (4 H,

m, C(4′)H_2 and C(9′)H_2), 3.87 (1 H, dd, $J = 4.0$, 6.1 Hz, C(2′)H), 4.35 (1 H, t, $J = 4.4$ Hz, C(7′)H); δ_C (500 MHz; D_2O) 26.1 (C8′), 26.2 (C3′), 30.5 (C9′), 31.5 (C4′), 52.7 (C7′), 53.7 (C2′), 173.3 (C=O), 174.9 (C=O), 175.7 (C=O), 177.5 (C=O), m/z (ESI^+) 277.1. ($C_{10}H_{17}N_2O_7$ requires 277.1). This material was identical to a sample of L-Glu-γ-L-Glu prepared by solution methods (see Supplementary Information).

An identical procedure varying only in the number of cycles of coupling, capping, and deprotection was used to synthesize all other peptides of the series H-Glu-γ-Glu_n-γ-Glu-OH, $n = 0$–4.

Purification of poly(γ-L-glutamate) peptides

The crude TFA salts of the peptides were dissolved in ddH_2O to yield solutions with a concentration of ~12 mg per 50 μL. 50 μL of these solutions were then individually used for purification *via* semi-preparative RP-HPLC as follows:

L-Glutamyl-(γ-L-glutamate)$_2$ (γ-Glu$_3$). Semi-preparative RP-HPLC (Method 2) yielded 10.9 mg, 21.0 μmol, of the TFA salt of the tripeptide after lyophilization. δ_H (300 MHz; D_2O) 1.87 (2 H, m, C(8′)H_2 and C(13′)H_2), 2.07 (4 H, m, C(3′)H_2, C(8′)H_2, and C(13′)H_2), 2.33 (6 H, m, C(4′)H_2, C(9′)H_2, and C(14′)H_2), 3.93 (1 H, t, $J = 6.4$ Hz, C(2′)H), 4.23 (2 H, m, C(7′)H and C(12′)H); Semi-preparative RP-HPLC (Method 2), $t_r = 16.0$ min; m/z (ESI^+) 406.2 ($C_{15}H_{24}N_3O_{10}$ requires 406.2) 406 (23%), 304 (100), and 282 (54).

L-Glutamyl-(γ-L-glutamate)$_3$ (γ-Glu$_4$). Semi-preparative RP-HPLC (Method 3) yielded 8.4 mg, 13.0 μmol, of the TFA salt of the tetrapeptide after lyophilization. δ_H (300 MHz; D_2O) 1.96 (3 H, m, C(8′)H_2, C(13′)H_2, and C(18′)H_2), 2.17 (5 H, m, C(3′)H_2, C(8′)H_2, C(13′)H_2, and C(18′)H_2), 2.45 (8 H, m, C(4′)H_2, C(9′)H_2, C(14′)H_2, and C(19′)H_2), 3.97 (1 H, t, $J = 6.4$ Hz, C(2′)H), 4.32 (2 H, m, C(7′)H and C(12′)H), 4.38 (1 H, m, C(17′)H); Semi-preparative RP-HPLC (Method 3), $t_r = 5.7$ min; m/z (ESI^+) 535.3 ($C_{20}H_{31}N_4O_{13}$ requires 535.2) 557 (20%), and 535 (100).

L-Glutamyl-(γ-L-glutamate)$_4$ (γ-Glu$_5$). Semi-preparative RP-HPLC (Method 4) yielded 8.9 mg, 11.4 μmol, of the TFA salt of the pentapeptide after lyophilization. δ_H (300 MHz; D_2O) 1.96 (4 H, m, C(8′)H_2, C(13′)H_2, C(18′)H_2, and C(23′)H_2), 2.17 (6 H, m, C(3′)H_2, C(8′)H_2, C(13′)H_2, C(18′)H_2, and C(23′)H_2), 2.45 (10 H, m, C(4′)H_2, C(9′)H_2, C(14′)H_2, C(19′)H_2, and C(24′)H_2), 3.97 (1 H, t, $J = 6.4$ Hz, C(2′)H), 4.32 (3 H, m, C(7′)H, C(12′)H, and C(17′)H), 4.39 (1 H, m, C(22′)H); Semi-preparative RP-HPLC (Method 4), $t_r = 10.7$ min; m/z (ESI^+) 664.4 ($C_{25}H_{38}N_5O_{16}$ requires 664.2) 664(100%).

L-Glutamyl-(γ-L-glutamate)$_5$ (γ-Glu$_6$). Semi-preparative RP-HPLC (Method 4) yielded 7.7 mg, 8.5 μmol, of the TFA salt of the hexapeptide after lyophilization. δ_H (300 MHz; D_2O) 1.96 (5 H, m, C(8′)H_2, C(13′)H_2, C(18′)H_2, C(23′)H_2, and C(28′)H_2), 2.17 (7 H, m, C(3′)H_2, C(8′)H_2, C(13′)H_2, C(18′)H_2, C(23′)H_2, and C(28′)H_2), 2.46 (12 H, m, C(4′)H_2, C(9′)H_2, C(14′)H_2, C(19′)H_2, C(24′)H_2, and C(29′)H_2), 3.96 (1 H, t, $J = 6.4$ Hz, C(2′)H), 4.33 (4 H, m, C(7′)H, C(12′)H, C(17′)H, and C(22′)H), 4.39 (1 H, m, C(27′)H); Semi-preparative RP-HPLC (Method 4), $t_r = 11.4$ min; m/z (ESI^+) 793.5 ($C_{30}H_{45}N_6O_{19}$ requires 793.3) 794 (22%), and 793 (100).

5,10-Dideaza-5,6,7,8-tetrahydropteroylglutamyl-γ-glutamates (DDAH$_4$PteGlu$_n$, n = 1–6) (1–6). An aqueous solution of the L-glutamate or poly-γ-glutamate (γ-Glu_{2-6}) was placed into a 10 × 75 mm test tube and concentrated to dryness on a vacuum centrifuge overnight at ambient temperature. When the tube was removed from the vacuum, a small, dry stir bar was placed in the tube and it was immediately sealed with a rubber septum. The tube was then gently flushed for 15 min with a stream of dry Ar introduced with a needle through the septum. The vent was then removed and the Ar line was replaced with an Ar-filled balloon. A solution consisting of (6*R*)-, or (6*S*)-5,10-dideazatetrahydropteroyl azide·HCl (**9**) (2 equiv.) in anhydrous DMSO was added to the tube with stirring followed by Et_3N (1 equiv. for each COOH of the amino acid or peptide, 1 equiv. for the amine salt (if applicable) of the amino acid or peptide, and 4 equiv. for **9**). The reaction was monitored by HPLC and stopped after 2 days by the addition of aqueous NH_4HCO_3 buffer (pH 8.1). The reaction solution was then concentrated on a vacuum centrifuge overnight with heating (35–40 °C) for product analysis (HPLC) followed by purification by size-exclusion chromatography. All DDAH$_4$PteGlu$_{2-6}$ compounds were further purified by semi-preparative RP-HPLC, as detailed below, unless otherwise noted. Product yields were determined by UV absorption (272 nm, 0.1 M NaOH, $\varepsilon = 11\,700\ M^{-1}\ cm^{-1}$).[10]

(6*R*)-5,10-Dideaza-5,6,7,8-tetrahydrofolic acid, (6*R*)-DDAH$_4$-PteGlu$_1$ (6*R*-1). Yield, 87%; λ_{max} (0.1 M NaOH)/nm 242 and 272; $[\alpha]_D = -29.3$ (0.1 M NaOD in D_2O) ($[\alpha]_D = -27.2$ (0.1 M NaOD in D_2O, from an authentic sample of (6*R*)-DDAH$_4$PteGlu$_1$–Na); lit.,[10] $[\alpha]_D = -21.1$ (1 N NaOH in methanol, from the *in situ* saponification of the *d*-10-(+)-camphorsulfonic acid salt of (6*R*)-DDAH$_4$PteGlu$_1$ diethyl ester)); δ_H (500 MHz; 0.1 M NaOD/D_2O) 1.65 (2H, dd, $J = 7.6$, 15.0 Hz, C(10)H_2), 1.79 (1 H, m, C(6)H), 2.01 (2 H, dd, $J = 8.9$, 15.4 Hz, C(5)H_2, C(3′)H_2), 2.15 (1 H, m, C(3′)H_2), 2.30 (2 H, dd, $J = 7.6$, 7.9 Hz, C(4′)H_2), 2.58 (1 H, dd, $J = 4.9$, 15.6 Hz, C(9)H_2), 2.79 (2 H, m, C(5)H_2 and C(9)H_2), 2.89 (1 H, m, C(7)H_2), 3.28 (1 H, br d, $J = 10.2$ Hz, C(7)H_2), 4.31 (1 H, m, C(2′)H), 7.41 (2 H, d, $J = 7.7$ Hz, C(12)H and C(16)H), 7.74 (2 H, d, $J = 7.7$ Hz, C(13)H and C(15)H); δ_C (500 MHz; 0.1 M NaOD/D_2O) 26.3, 28.9, 31.5, 33.0, 34.7, 45.7, 56.4, 87.5, 127.8, 129.2, 131.4, 148.1, 161.0, 161.6, 170.6, 174.1, 179.4, 182.7; m/z (ESI^+) 444.1873 (M + H^+. $C_{21}H_{26}N_5O_6$ requires 444.1883) 445 (25%), and 444 (100); Ion-pair HPLC, $t_r = 18.4$ min. Spectral data (UV/vis, ^1H NMR, and ^{13}C NMR) are identical to those obtained with an authentic sample of (6*R*)-DDAH$_4$PteGlu$_1$.

(6*S*)-5,10-Dideaza-5,6,7,8-tetrahydrofolic acid, (6*S*)-DDAH$_4$-PteGlu$_1$ (6*S*-1). Yield, 92%; λ_{max} (0.1 M NaOH)/nm 242 and 272; $[\alpha]_D = +29.2$ (0.1 M NaOD in D_2O) (lit.,[10] $[\alpha]_D = +31.1$ (1 N NaOH in methanol, from the *in situ* saponification of the *d*-10-(+)-camphorsulfonic acid salt of (6*S*)-DDAH$_4$PteGlu$_1$ diethyl ester); δ_H (500 MHz; 0.1 M NaOD/D_2O) 1.65 (2H, dd, $J = 6.7$, 14.3 Hz, C(10)H_2), 1.79 (1 H, m, C(6)H), 2.02 (2 H, dd, $J = 7.4$, 15.4 Hz, C(5)H_2, C(3′)H_2), 2.14 (1 H, m, C(3′)H_2), 2.30 (2 H, dd, $J = 6.7$, 7.9 Hz, C(4′)H_2), 2.58 (1 H, m, C(9)H_2), 2.79 (2 H, m, C(5)H_2 and C(9)H_2), 2.89 (1 H, dd, C(7)H_2), 3.28 (1 H, br d, $J = 11.7$ Hz, C(7)H_2), 4.31 (1 H, m, C(2′)H), 7.42 (2 H, d, $J = 8.2$ Hz, C(12)H and C(16)H), 7.74 (2 H, d, $J = 8.2$ Hz, C(13)H and C(15)H); δ_C (500 MHz; 0.1 M NaOD/D_2O) 26.3, 28.8, 31.4, 32.9, 34.7, 45.7, 56.4, 87.4, 127.8, 129.1, 131.4, 148.0, 161.0, 161.6, 170.6, 174.1, 179.4, 182.7; m/z (ESI^+) 444.1879 (M + H^+. $C_{21}H_{26}N_5O_6$ requires 444.1883) 445 (23%), and 444 (100); Ion-pair HPLC, $t_r = 17.7$ min.

(6*R*)-[^{14}C]5,10-Dideaza-5,6,7,8-tetrahydrofolic acid, (6*R*)-DDAH$_4$Pte[^{14}C]Glu$_1$. A 10 mL solution (ethanol–H_2O, 2 : 98) containing 1.0 mCi of L-[U-^{14}C]glutamic acid was evaporated to dryness on a vacuum centrifuge. This residue was used in a reaction with 6*R*-**9** generally as described above but with special precautions in place to prevent the inadvertent release of radioactive material. Two purifications by size-exclusion chromatography were required to obtain product of the desired radiochemical purity. Yield, 62%; Ion-pair HPLC, t_r = 17.5–18.5 min.; Purity, 96%; Specific activity = 249 Ci mol^{-1}.

(6*R*)-5,10-Dideaza-5,6,7,8-tetrahydropteroyl-L-glutamate-γ-L-glutamate (6*R*-2). Crude **γ-Glu$_2$** was used for this reaction. Purified using semi-preparative RP-HPLC (Method 5), t_r = 20.0 min. Yield, 39%; λ_{max} (0.1 M NaOH)/nm 242 and 272; m/z (ESI^+) 573.2 (M + H^+. $C_{26}H_{33}N_6O_9$ requires 573.2); m/z (ESI^+)

573.2305 (M + H$^+$. $C_{26}H_{33}N_6O_9$ requires 573.2309) 574 (32%), 573 (100), 349 (21), and 305 (48); Ion-pair HPLC, $t_r = 22.2$ min.

(6*S*)-5,10-Dideaza-5,6,7,8-tetrahydropteroyl-L-glutamate-γ-L-glutamate (6*S*-2). Crude **γ-Glu$_2$** was used for this reaction. Purification was by size-exclusion chromatography only. Yield, 31%; λ_{max} (0.1 M NaOH)/nm 242 and 272; *m/z* (ESI$^+$) 573.2324 (M + H$^+$. $C_{26}H_{33}N_6O_9$ requires 573.2309) 574 (29%), 573 (100), 305 (50), 274 (22), and 261 (34); Ion-pair HPLC, $t_r = 20.8$ min.

(6*R*)-5,10-Dideaza-5,6,7,8-tetrahydropteroyl-L-glutamate-(γ-L-glutamate)$_2$ (6*R*-3). Purified using semi-preparative RP-HPLC (Method 5), $t_r = 15.0$ min. Yield, 78%; λ_{max} (0.1 M NaOH)/nm 242 and 272; δ_H (500 MHz; 0.1 M NaOD/D_2O; numbering system, see Supplementary Information, Scheme S3) 1.72 (2 H, m, C(10)H$_2$), 1.89 (3 H, m, C(6)H, C(8′)H$_2$, and C(13′)H$_2$), 2.07 (5 H, m, C(5)H$_2$, C(3′)H$_2$, C(8′)H$_2$, and C(13′)H$_2$), 2.23 (2 H, dd, $J = 7.8$, 8.3 Hz, C(9′)H$_2$), 2.31 (2 H, dd, $J = 7.7$, 8.2 Hz, C(4′)H$_2$), 2.48 (2 H, dd, $J = 6.4$, 7.8 Hz, C(14′)H$_2$), 2.63 (1 H, m, C(9)H$_2$), 2.84 (2 H, m, C(5)H$_2$ and C(9)H$_2$), 2.95 (1 H, m, C(7)H$_2$), 3.34 (1 H, br d, $J = 11.5$ Hz, C(7)H$_2$), 4.12 (2 H, m, C(7′)H and C(12′)H), 4.40 (1 H, dd, $J = 4.5$, 8.9 Hz, C(2′)H), 7.46 (2 H, d, $J = 7.9$ Hz, C(12)H and C(16)H), 7.76 (2 H, d, $J = 7.9$ Hz, C(13)H and C(15)H); *m/z* (ESI$^+$) 724.2527 (M + Na$^+$. $C_{31}H_{39}N_7NaO_{12}$ requires 724.2554) 702 (100%); Ion-pair HPLC, $t_r = 29.3$ min.

(6*R*)-5,10-Dideaza-5,6,7,8-tetrahydropteroyl-L-glutamate-(γ-L-glutamate)$_3$ (6*R*-4). Purified using semi-preparative RP-HPLC (Method 6), $t_r = 12.0$ min. Yield, 59%; λ_{max} (0.1 M NaOH)/nm 242 and 272; *m/z* (ESI$^+$) 853.2989 (M + Na$^+$. $C_{36}H_{46}N_8NaO_{15}$ requires 853.2980) 832 (20%), 831 (100), and 427 (50); Ion-pair HPLC, $t_r = 37.0$ min.

(6*R*)-5,10-Dideaza-5,6,7,8-tetrahydropteroyl-L-glutamate-(γ-L-glutamate)$_4$ (6*R*-5). Purified using semi-preparative RP-HPLC (Method 7), $t_r = 13.5$ min. Yield, 53%; λ_{max} (0.1 M NaOH)/nm 242 and 272; *m/z* (ESI$^+$) 982.3409 (M + Na$^+$. $C_{41}H_{53}N_9NaO_{18}$ requires 982.3406) 960 (20%), 492 (30), 491 (63), and 381 (100); Ion-pair HPLC, $t_r = 43.4$ min.

(6*R*)-5,10-Dideaza-5,6,7,8-tetrahydropteroyl-L-glutamate-(γ-L-glutamate)$_5$ (6*R*-6). Purified using semi-preparative RP-HPLC (Method 8), $t_r = 15.5$ min. Yield, 55%; λ_{max} (0.1 M NaOH)/nm 242 and 272; *m/z* (ESI$^+$) 1111.3868 (M + Na$^+$. $C_{46}H_{60}N_{10}NaO_{21}$ requires 1111.3832) 1089 (20), 556 (100), 545 (30), and 381 (41); Ion-pair HPLC, $t_r = 48.4$ min.

Preparation of DDAH$_4$PteGlu$_n$ solutions

Each DDAH$_4$PteGlu$_n$ was dissolved in 1–2 mL of 20–100 mM NaOH. The resulting solutions were filtered through a spin-filter. All solutions were then stored at −20 °C. Concentrations of the solutions were determined based on absorbance at 272 nm (0.1 M NaOH, $\varepsilon = 11{,}700$ M^{-1} cm^{-1}).[10] All solutions of DDAH$_4$PteGlu$_n$ were freshly prepared and purity confirmed by HPLC. Extended storage (>2 months, −20 °C) of solutions with [NaOH] > 20 mM led to partial hydrolysis of the polyglutamate chain yielding a mixture of shorter chain compounds.

hFPGS Assays

Total glutamate incorporation.

Determination of steady-state kinetic constants[49,55]. *General conditions*: Final concentrations of 100 mM Tris (pH 8.85), 10 mM $MgCl_2$, 20 mM KCl, 10 mM $NaHCO_3$, 0.5 mg mL^{-1} bovine serum albumin, 5 mM ATP, 2 mM L-[^{3}H]glutamate (specific activity ~2.6 cpm pmol^{-1}), 0–300 μM DDAH$_4$PteGlu$_n$, 14 nM hFPGS, 250 μL reaction volume, 60 min reaction time, and 37 °C. The solution was incubated at 37 °C for 5 min prior to addition of partially purified hFPGS expressed in either *E. coli* ($n = 1$–2) or bacculovirus-infected SF9 insect cells ($n = 3$–6) to initiate the reaction. Reactions were carried out in 1.5 mL, silanized Eppendorf tubes and were stopped by the addition of 1 mL of ice-cold buffer consisting of 5 mM glutamate, pH 7.5.

Assay products were purified with DEAE-cellulose (DE-52) ion-exchange chromatography using a buffer consisting of 10 mM Tris, and 110 mM NaCl, conductivity ~11.5 mS, at pH 7.5 to remove unincorporated [^{3}H]glutamate. Folate products were eluted with 0.1 M HCl. The amount of tritium incorporation into the folate products was determined by liquid scintillation counting. All reactions were carried out in duplicate and the blank reactions lacked the folate substrate.

Analysis of product formation. *General conditions*: As above, except for final concentrations of 20 mM $MgCl_2$, 5 mM dithiothreitol, 10 mM ATP, and 5 mM glutamate. The concentrations of (6*R*)-DDAH$_4$Pte[^{14}C]Glu$_1$ utilized were 2.5, 25, or 250 μM with specific activities of 249, 24.9, and 2.49 Ci mol^{-1} respectively. A 5 min reaction time was utilized with a final [hFPGS] = 1 μM and volume of 80 μL.

The solution was incubated at 37 °C for 5 min prior to reaction initiation by addition of purified hFPGS. The reactions were stopped by addition of 50% w/v trichloroacetic acid, with mixing, to a final volume of 5% w/v. For the control reaction, trichloroacetic acid was added immediately prior to the addition of hFPGS and analysis showed no product formation. The tubes were stored at −80 °C. The samples were clarified prior to HPLC analysis by centrifugation (16 000*g*, 10 min).

Ion-pair HPLC method: A portion (75 μL) of each sample was analyzed using the ion-pair HPLC method described above except fractions (30 s) were collected over the range $t_r = 10$–60 min.

Liquid scintillation counting method: The 30 s fractions were collected directly into 5.5 mL plastic scintillation vials. Bio-Safe II scintillation cocktail (4.0 mL) was added to each vial before capping and mixing by vortexing. Radioactivity (DPM) of each fraction was determined by liquid scintillation counting.

Acknowledgements

This research was supported in part by grants from the National Cancer Institute, CA 28097 (J.K.C.), CA43500 (J.J.M.), and CA16056 (Roswell Park Cancer Center Support Grant). J.W.T. was a trainee of the Michigan Chemistry-Biology Interface Training Program, supported in part by a grant from the National Institutes of General Medical Sciences (GM008597). J.W.T. was the recipient of a Fred W. Lyons Fellowship from the College of Pharmacy, University of Michigan, and a fellowship from the American Foundation for Pharmaceutical Education. We thank Dr Chuan Shih, Eli Lilly & Co, Indianapolis, IN, for the generous gift of (6*R*)-DDAH$_4$PteGlu$_1$ (Lometrexol™), (6*RS*)-DDAH$_4$PteGlu$_2$, and (6*RS*)-DDAH$_4$PteGlu$_5$ used in initial experiments. In addition, we gratefully acknowledge the contribution to this research of Dr Michael J. Lovdahl and Anne Akin, Analytical Development Department, Pfizer Global Research and Development, Ann Arbor, MI, for carrying out the separation of 6*R*-**7** and 6*S*-**7** by chiral HPLC on a preparative scale. We thank Sanyo Tsai for aid in the preparation of the poly-γ-glutamate peptides, William Haile for partial purification of hFPGS, Prof. Richard Moran for a sample of purified hFPGS, Prof. Edwin Vedejs for the loan of an analytical chiral HPLC column, and Prof. Bruce Palfey for assistance with the kinetic modeling studies.

References and notes

1 J. J. McGuire and J. R. Bertino, *Mol. Cell. Biochem.*, 1981, **38**, 19–48.
2 J. J. McGuire, and J. K. Coward, in *Folates and Pterins*, ed. R. L. Blakley and S. J. Benkovic, John Wiley & Sons, New York, 1984, pp. 135–190.
3 B. Shane, *Vitamins and Hormones – Advances in Research and Applications*, 1989, **45**, 263–335.

4 L. G. Mendelsohn, J. F. Worzalla, and J. M. Walling, in *Antifolate Drugs in Cancer Therapy*, ed. A. L. Jackman, 1999, Humana, Totowa, NJ, pp. 261–280.
5 J. Adams and P. J. Elliott, *Oncogene*, 2000, **19**, 6687–6692.
6 J. J. McGuire, *Curr. Pharm. Des.*, 2003, **9**, 2593–2613.
7 W. T. Purcell and D. S. Ettinger, *Curr. Oncol. Rep.*, 2003, **5**, 114–125.
8 G. P. Beardsley, B. A. Moroson, E. C. Taylor and R. G. Moran, *J. Biol. Chem.*, 1989, **264**, 328–333.
9 G. P. Beardsley, E. C. Taylor, G. B. Grindey, and R. G. Moran, in *Chemistry and Biology of the Pteridines 1986*, ed. B. A. Cooper and V. M. Whitehead, Walter de Gruyter & Co., Berlin, 1986, pp. 953–957.
10 R. G. Moran, S. W. Baldwin, E. C. Taylor and C. Shih, *J. Biol. Chem.*, 1989, **264**, 21047–21051.
11 G. Pizzorno, J. A. Sokoloski, A. R. Cashmore, B. A. Moroson, A. D. Cross and G. P. Beardsley, *Mol. Pharmacol.*, 1991, **39**, 85–89.
12 P. C. Sanghani and R. G. Moran, *Protein Expression Purif.*, 2000, **18**, 36–45.
13 L. L. Habeck, S. H. Chay, R. C. Pohland, J. F. Worzalla, C. Shih and L. G. Mendelsohn, *Cancer Chemother. Pharmacol.*, 1998, **41**, 201–209.
14 E. C. Taylor, P. J. Harrington, S. R. Fletcher, G. P. Beardsley and R. G. Moran, *J. Med. Chem.*, 1985, **28**, 914–921.
15 L. L. Habeck, L. G. Mendelsohn, C. Shih, E. C. Taylor, P. D. Colman, L. S. Gossett, T. A. Leitner, R. M. Schultz, S. L. Andis and R. G. Moran, *Mol. Pharmacol.*, 1995, **48**, 326–333.
16 S. W. Baldwin, A. Tse, L. S. Gossett, E. C. Taylor, A. Rosowsky, C. Shih and R. G. Moran, *Biochemistry*, 1991, **30**, 1997–2006.
17 H. M. Faessel, H. K. Slocum, R. C. Jackson, T. J. Boritzki, Y. M. Rustum, M. G. Nair and W. R. Greco, *Cancer Res.*, 1998, **58**, 3036–3050.
18 J. J. McGuire, in *Antifolate Drugs in Cancer Therapy*, ed. A. L. Jackman, 1999, Humana, Totowa, NJ, pp. 339–363.
19 E. Liani, L. Rothem, M. A. Bunni, C. A. Smith, G. Jansen and Y. G. Assaraf, *Int. J. Cancer*, 2003, **103**, 587–599.
20 E. C. Taylor, *J. Heterocycl. Chem.*, 1990, **27**, 1–12.
21 I. Durucasu, *Heterocycles*, 1993, **35**, 1527–1545.
22 E. C. Taylor, G. S. K. Wong, S. R. Fletcher, P. J. Harrington, G. P. Beardsley, and C. J. Shih, in *Chemistry and Biology of Pteridines 1986*, ed. B. A. Cooper and V. M. Whitehead, Walter de Gruyter & Co., Berlin, 1986, pp. 61–64.
23 C. J. Barnett, T. M. Wilson, S. R. Wendel, M. J. Winningham and J. B. Deeter, *J. Org. Chem.*, 1994, **59**, 7038–7045.
24 J. Luo, M. D. Smith, D. A. Lantrip, S. Wang and P. L. Fuchs, *J. Am. Chem. Soc.*, 1997, **119**, 10004–10013.
25 N. Valiaeva, D. Bartley, T. Konno and J. K. Coward, *J. Org. Chem.*, 2001, **66**, 5146–5154.
26 E. C. Taylor, R. Chaudhari and K. Lee, *Invest. New Drugs*, 1996, **14**, 281–285.
27 A. D. Cross, H. Morimoto, P. G. Williams and G. P. Beardsley, *J. Labelled Compd. Radiopharm.*, 1991, **29**, 753–763.
28 C. L. Krumdieck and C. M. Baugh, *Biochemistry*, 1969, **8**, 1568–1572.
29 J. Meienhofer, P. M. Jacobs, H. A. Godwin and I. H. Rosenberg, *J. Org. Chem.*, 1970, **35**, 4137–4140.
30 M. R. Mejillano, H. Jahansouz, T. O. Matsunaga, G. L. Kenyon and R. H. Himes, *Biochemistry*, 1989, **28**, 5136–5145.
31 H. A. Godwin, I. H. Rosenberg, C. R. Ferenz, P. M. Jacobs and J. Meienhofer, *J. Biol. Chem.*, 1972, **247**, 2266–2271.
32 J. K. Coward, K. N. Parameswaran, A. R. Cashmore and J. R. Bertino, *Biochemistry*, 1974, **13**, 3899–3903.
33 C. N. C. Drey and G. P. Priestly, *J. Chem. Res.*, 1979, **2**, 3055–3071.
34 J. R. Piper, G. S. McCaleb and J. A. Montgomery, *J. Med. Chem.*, 1983, **26**, 291–294.
35 L. D'Ari and J. C. Rabinowitz, *Methods Enzymol.*, 1985, **113**, 169–182.
36 W. P. Jencks, and J. Regenstein, in *CRC Handbook of Biochemistry and Molecular Biology*, ed. G. D. Fasman, 1975, CRC Press, Inc., Boca Raton, FL, pp. 305–351.
37 G. X. B. Ma, R. A. Batey, S. D. Taylor, G. Hum and J. B. Jones, *Synth. Commun.*, 1997, **27**, 2445–2453.
38 W. Chan, and P. White, *Fmoc Solid Phase Peptide Synthesis: A Practical Approach*, Oxford University Press Inc., New York, 2000.
39 M. Dixon, and E. C. Webb, *Enzymes* (3rd edn), Academic Press, New York, 1979. Eqn (2) is valid under our assay conditions of fixed, saturating concentrations of ATP and glutamate.
40 V. Leskovac, *Comprehensive Enzyme Kinetics*, Kluwer Academic/Plenum Publishers, New York, 2003.
41 X. Sun, A. L. Bognar, E. N. Baker and C. A. Smith, *Proc. Natl. Acad. Sci. U. S. A.*, 1998, **95**, 6647–6652.
42 X. Sun, J. A. Cross, A. L. Bognar, E. N. Baker and C. A. Smith, *J. Mol. Biol.*, 2001, **310**, 1067–1078.
43 M. Mathieu, G. Debousker, S. Vincent, F. Viviani, N. Bamas-Jacques and V. Mikol, *J. Biol. Chem.*, 2005, **280**, 18916–18922.
44 Additional reducing agent was not included in these reactions, as early experiments with hFPGS expressed in *E. coli* indicated no measurable effect of the presence of reducing agent on enzyme activity or product distribution. However, the reactions that utilized enzyme expressed in *E. coli* had a final concentration of 4 mM 2-mercaptoethanol due to its presence in the enzyme storage buffer. In contrast, the reactions in which enzyme expressed in SF-9 insect cells had been used, the final concentration of 2-mercaptoethanol was 0.4 mM. Subsequently, it was determined that additional reducing agent (100 mM 2-mercaptoethanol or 5 mM dithiothreitol) increased the chain-length of the polyglutamate products produced only for the hFPGS expressed in SF-9 insect cells. This observation suggests that the addition of reducing agent to the assays shown in Fig. 3 would intensify the observed substrate inhibition.
45 L. Chen, H. Qi, J. Korenberg, T. A. Garrow, Y. J. Choi and B. Shane, *J. Biol. Chem.*, 1996, **271**, 13077–13087.
46 R. Banerjee, J. J. McGuire, B. Shane and J. K. Coward, *Biochemistry*, 1988, **27**, 9062–9070.
47 J. W. Tomsho, *Ph.D. dissertation*, University of Michigan, Ann Arbor, MI, 2005.
48 I. H. Segel, *Enzyme Kinetics*, John Wiley & Sons, New York, 1975.
49 J. J. McGuire, P. Hsieh, J. K. Coward and J. R. Bertino, *J. Biol. Chem.*, 1980, **255**, 5776–5788.
50 A. Gangjee, J. Yu, R. L. Kisliuk, W. H. Haile, G. Sobrero and J. J. McGuire, *J. Med. Chem.*, 2003, **46**, 591–600.
51 M. M. Bradford, *Anal. Biochem.*, 1976, **72**, 248–254.
52 P. J. Bagley and J. Selhub, *Methods Enzymol.*, 1997, **281**, 16–25.
53 C. J. Barnett and T. M. Wilson, *Tetrahedron Lett.*, 1989, **30**, 6291–6294.
54 C. J. Barnett, and T. M. Wilson, in *Chemistry and Biology of Pteridines 1989*, ed. H.-C. Curtius, S. Ghisla and N. Blau, Walter de Gruyter, Berlin, 1990, pp. 102–105.
55 J. J. McGuire, P. Hsieh, J. K. Coward, and J. R. Bertino, in *Folyl and Antifolyl Polyglutamates*, ed. I. D. Goldman, B. A. Chabner, and J. R. Bertino, Plenum Press, New York, 1983, pp. 199–214.